

# Reduce Computational Complexity for Convolutional Layers by Skipping Zeros

Zhiyi Zhang, Pengfei Zhang, Zhuopin Xu, Qi Wang

**Abstract**—Deep neural networks rely on parallel processors for acceleration. To design operators for them, it requires not only good algorithm to reduce complexity, but also sufficient utilization of hardwares. Convolutional layers mainly contain 3 kinds of operators: convolution in forward propagation, deconvolution and dilated-convolution in backward propagation. When executing these operators, 0s are always added to tensors, causing redundant calculations. This paper gives *C-K-S* algorithm (*ConvV2*, *KS-deconv*, *Sk-dilated*), which skips these 0s in two ways: trim the filters to exclude padded 0s; transform sparse tensors to dense tensors, to avoid inserted 0s in deconvolution and dilated-convolution. In contrast to regular convolution, deconvolution is hard to accelerate due to its complicity. This paper provides high-performance GPU implementations of *C-K-S*, and verifies their effectiveness with comparison to PyTorch. According to the experiments, *C-K-S* has advantages over PyTorch in certain cases, especially in deconvolution on small feature-maps. Further enhancement of *C-K-S* can be done by making full optimizations oriented at specific GPU architectures.

**Index Terms** — convolutional neural networks (CNNs), deconvolution, dilated-convolution, parallel computing, accelerator architecture.

## I. INTRODUCTION

Convolutional layers (conv-layers) are generally used in deep neural networks (DNNs) [2]-[6], with advantages of parameter sharing, sparse interactions and equivariant representations [1]. In conv-layers, 0s are generally added to tensors for specific purposes, like generating output-features with expected size, or solving gradients of input-features and filters (convolutional kernel). These 0s causes redundant calculations (0-calculations), so the computational complexity can be reduced by skipping them.

Conv-layers briefly requires 3 kinds of convolutional operators: convolution in forward propagation, deconvolution (transposed convolution) and dilated-convolution in backward propagation. These 3 operators take the most resources in training convolutional neural networks (CNNs), so it's always a key issue to optimize them [7]-[9]. The efficient implementations of conv-layers are usually based on parallel processors, such as GPU and FPGA, for their superiority in accelerating intensive computations. In a word, for DNNs, good algorithms in theory, and the adaptability to hardwares are both important.

To exclude 0-calculations in conv-layers, this paper presents *C-K-S* algorithm (*ConvV2*, *KS-deconv*, *Sk-dilated*) with its efficient GPU implementations. The *C-K-S* has been applied to Dragon-Alpha [10] [22], which spends less time and memory than PyTorch [11] to train some typical DNNs [2]-[5] on Cifar10, so this paper can be regarded as a summary of Dragon-Alpha's convolution techniques. This paper uses 'is' for 'features' and 'filters' to see them as a whole; and uses  $n$  to refer input data size, to more simply express time-complexity. The relevant parameter notations are in Table I.

---

This research was supported by National Natural Science Foundation of China (No. 32070399); Anhui Science and Technology Major Project (No. 202103a06020014), the Chinese Academy of Sciences-Henan Province Achievement transfer and Transformation Project (No. 2022208); Hefei Science and Technology Project (No. 2021GJ065).

Zhiyi Zhang, Pengfei Zhang, Zhuopin Xu and Qi Wang are with the HFIFPS (Hefei Institutes of Physical Science, Chinese Academy of Sciences), Hefei, China. Zhiyi Zhang is also with USTC (University of Science and Technology of China), Hefei, China.

Zhiyi Zhang (email: gilgamesh@mail.ustc.edu.cn) is the first author, Pengfei Zhang (email: pfzhang@aiofm.ac.cn) is the second author, Zhuopin Xu (xuzp@iim.ac.cn) is the third author, and Qi Wang (email: wangqi@ipp.ac.cn) is the corresponding author.

TABLE I  
PARAMETER NOTATIONS

Notation	Explanation
*	Scalar-multiply or Convolution
$\times$	Cartesian-product or matrix-multiply
$\odot$	Element-wise multiply
$\langle \cdot \rangle$	Matrix or Vector
<b>in-range-of</b>	Return true if an index is within the range of a tensor, otherwise return false
$X_{n, ih, iw, ic}$	An element with index of the input-features $X$
$Y_{n, oh, ow, ic}$	An element with index of the output-features $Y$
$W_{oc, fh, fw, ic}$	An element with index of the filters $W$
$I_H \setminus I_W$	Height \ Width of the input-features $X$
$O_H \setminus O_W$	Height \ Width of the output-features $Y$
$F_H \setminus F_W$	Height \ Width of the filters $W$
$N \setminus I_C \setminus O_C$	BatchSize \ Input channels \ Output channels
$sh \setminus sw$	Stride on height \ width axis in forward propagation
$ph \setminus pw$	Padding on height \ width axis in forward propagation

## II. BACKGROUND

### A. 0-Calculations Caused By Padding

To generate the output-features  $Y$  with expected size in conv-layers, the input-features  $X$  are usually padded with certain 0s (Fig. 3). In many DNNs, due to downsampling, the size of feature-maps decreases with going deeper. Under this circumstance, the proportion of the padded 0s in  $X$  is small in shallow layers, but could be big enough in deeper layers to results in a non-negligible amount of redundant calculation. As shown in Fig. 1, the red curve represents the proportion of padded 0s in  $X$ , and the blue curve indicates the proportion of 0-calculations in the total amount. For 2D-convolution with padding 1 and  $3 \times 3$  filters, the values of red and blue curves become bigger, as the size of square feature-map ( $F \times F$ ) decreases. To avoid such 0-calculations, *ConvV2* trims the filters for each patch of  $X$  so that all padded 0s are excluded.

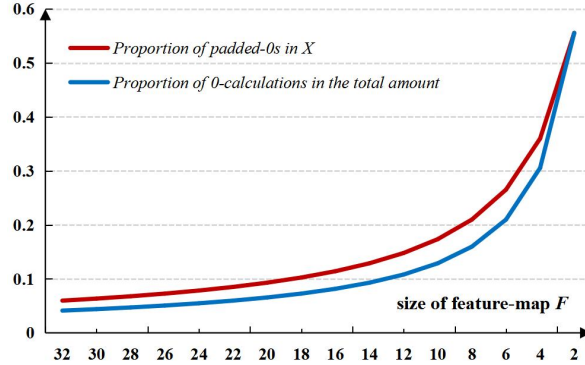


Fig. 1. padding causes more 0-calculations on smaller feature-maps.

### B. 0-Calculations Caused by Sparse Tensors

Convolution and deconvolution are a pair of reciprocal operators. Usually, convolution is for downsampling to reduce feature-size, while deconvolution is for up-sampling to enlarge feature-size. If convolution generates the output-features  $Y$  in forward propagation (1), deconvolution will be used to find the gradient of the input-features  $X$  in backward propagation (2), and vice versa. Dilated-convolution is used for finding the gradient of the filters  $W$  (3).

$$Y = conv_{2D}(X, W) \quad (1)$$

$$\nabla X = deconv_{2D}(\nabla Y, W^{rot180}) \quad (2)$$

$$\nabla W = dilated\_conv_{2D}(X, \nabla Y) \quad (3)$$

When stride of convolution is greater than 1, (stride - 1) 0s will be inserted between each element of  $\nabla Y$ , in order to find  $\nabla X$  and  $\nabla W$  through deconvolution and dilated-convolution. Such 0s account for a big proportion in  $\nabla Y$  making it a sparse tensor, and lead to many 0-calculations. As shown in Fig.2, except for the necessary calculations with colored elements, the rest calculations are otiose. To avoid these 0-calculations, *KS-deconv* and *SK-dilated* transform  $\nabla Y$  back to dense tensor, through filter-reconstruction and leaping-element-access. They can be combined with *ConvV2* to have better performance especially on small feature-maps.

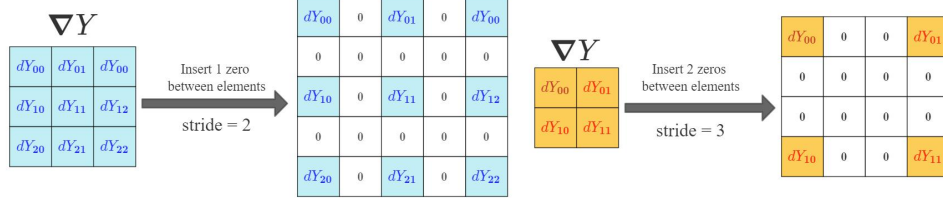


Fig. 2. Insert (stride - 1) 0s between adjacent elements of  $\nabla Y$ .

### C. Approaches to Implement 2D-Convolution

There are several approaches to implement 2D-convolution on GPU. The approach of A. Krizhevsky [21] is computing it directly, that's efficiency in some cases but poor in others. Compared to dense convolution, FFT-convolution has much smaller time-complexity in theory; but it needs lots of temporary memory to pad the filters the same size as input-feature-maps, and has lower performance in small-filter or big-stride cases. Y. Jia *et. al.* [20] lower 2D-convolution to matrix-multiply through *im2col* (Fig. 3). This approach has stable and good performance, and can be widely applied based on matrix acceleration libraries, but needs auxiliary memory to stored the unfolded tensors. CuDNN [8] optimizes this approach, by implicitly integrating *im2col* to *GEMM* (General Matrix Multiply) operators, to improve the speed without auxiliary memory.

The *direct* [21] and *implicit-GEMM* [8] approaches are referred to implement *C-K-S* on GPU. Since deconvolution and dilated-convolution are special kinds of convolution, it's feasible to implement them in a similar way to convolution.

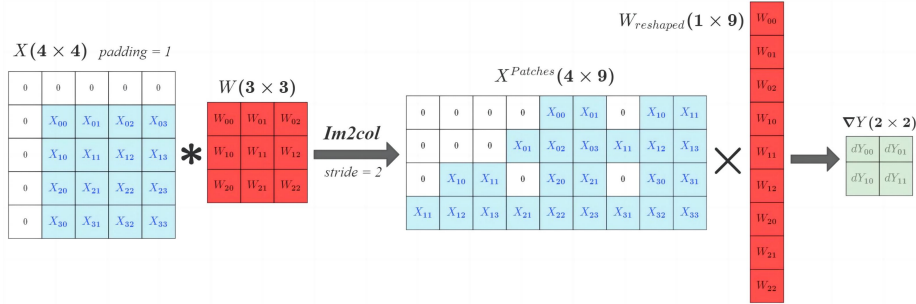


Fig. 3. Through *im2col*, the 2D-convolution  $X * W$  is transformed to matrix-multiply  $X^{Patches} \times W^{reshaped}$ . The time-complexity is 72, but only 52 calculations are necessary.

### D. Related Works

Related methods have been proposed [15]-[19] to avoid 0-calculations in deconvolution. Orosa *et. al.* [18] devise a compile-time computation scheduling for deconvolution, to avoid 0-calculations with minimal hardware overhead. J. Chang *et. al.* [15] propose the TDC method, to transform sparse deconvolution to dense convolution, and implement it on FPGA. K.Chang *et. al.* [16] and A. M. Vadakkevedu *et.al.* [17] decompose the convolutional kernel to multi smaller ones, to exclude 0-calculations. Cutlass [19] provides an implementation of *strided\_dgrad*, which skips 0-calculations by thread indices, but it may not be universally applicable since it's specific to the CUDA programming-model and architectures.

The kernel-decomposition ideas [15]-[17] are somewhere close to *KS-deconv*'s, but there exists some differences. Compared to the method of J.Chang *et. al.* [15], *KS-deconv* has lower time-complexity because of smaller decomposed kernels. In the work of K.Chang *et. al.* [16] and A. M. Vadakkevedu *et.al.* [17], their kernel-decomposition results are similar to *KS-deconv*'s in several specific cases, but there lacks explicit math formulas to make a general comparison. Besides, this work implements *KS-deconv* on different system architectures, and further combines it with *ConvV2*.

### III. 2D ALGORITHMS AND IMPLEMENTATIONS

The 2D-convolution in DNNs is with channels and batches, so the input-features  $\mathbf{X} \in \mathbb{R}^{N \times I_H \times I_W \times I_C}$ , output-features  $\mathbf{Y} \in \mathbb{R}^{N \times O_H \times O_W \times O_C}$  and filters  $\mathbf{W} \in \mathbb{R}^{O_C \times F_H \times F_W \times I_C}$  are all 4D tensors. *ConvV2* is described from the perspective of forward propagation, while *KS-deconv* and *Sk-dilated* are in a view of finding  $\nabla \mathbf{X}$  and  $\nabla \mathbf{W}$  in backward propagation. All pseudo code of algorithms are concentrated in section III.E.

#### A. ConvV2: Convolution with Trimmed Filters

To perform 2D-convolution,  $\mathbf{W}$  is used as a sliding window to generate patches of  $\mathbf{X}$  with padded 0s. For a specific patch, the padded 0s only appears at the edge, while the rest meaningful elements are all in the center. The start-position  $(fh_s, fw_s)$  of these meaningful elements is in the top-left corner, and the end-position  $(fh_e - 1, fw_e - 1)$  is in the down-right corner. *ConvV2* trims  $\mathbf{W}$  to only cover the meaningful part from the start-position to the end. Thus all padded 0s don't participate in the calculations, and the height and width of  $\mathbf{W}$  are reduced from  $(fh_e - fh_s) \times (fw_e - fw_s)$ , that obviously lowers time-complexity. As shown in Fig. 4,  $\mathbf{W}$  is trimmed from  $3 \times 3$  to  $2 \times 2$  for the selected patch; the time-complexity of *ConvV2* is 50, that's smaller than the 72 of normal convolution (Fig. 2). The pseudo code of *ConvV2* is in Algorithm 1.

Practically, *padding* is achieved by conditional-statements: to fetch an element with specific index, give its value if in range, but 0 if not. Such logical *padding* sacrifices a little speed, but significantly saves memory. Since all padded 0s are excluded in *ConvV2*, there is no conditional-statements for logical *padding*, which improves the efficiency. When  $\mathbf{X}$  is large enough, the dimension order of  $\mathbf{W}$  will be changed from  $O_C \times F_H \times F_W \times I_C$  to  $F_H \times F_W \times I_C \times O_C$  to improve the memory bandwidth, that brings about 5% increase on speed.

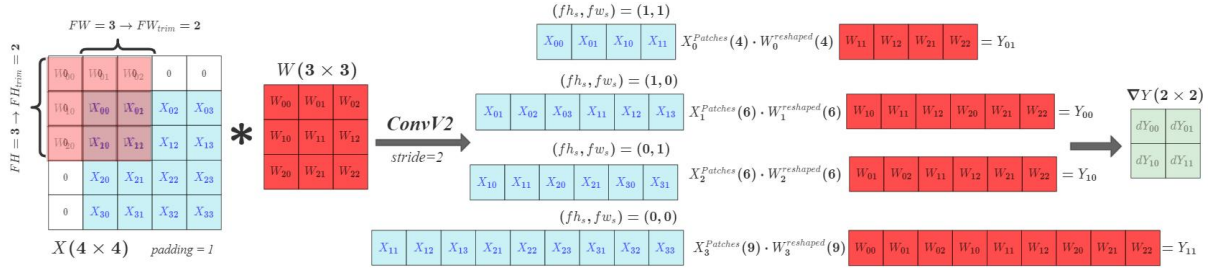


Fig. 4. *ConvV2* trims the filters to exclude all padded 0s.

#### B. KS-deconv: Kernel-Split Deconvolution

The *KS-deconv* is used for deconvolution with stride greater than 1. if stride is 1, the naive approach is simpler and faster, owing to the density of  $\nabla \mathbf{Y}$ . *KS-deconv* contains 3 stages, and its pseudo code is in Algorithm 2.

**Stage1** *kernel-split* (Fig.5): rotate  $\mathbf{W}$  180 degrees, then split  $\mathbf{W}$  to construct  $(sh * sw)$  smaller kernels with 2D indices. The shape of the  $(y, x)_{th}$  smaller kernel  $\mathbf{C}_{y, x}$  is  $O_C \times \left\lceil \frac{F_H - y}{sh} \right\rceil \times \left\lceil \frac{F_W - x}{sw} \right\rceil \times I_C$ . Concat all smaller kernels to a 6D tensor  $\mathbf{C} \in \mathbb{R}^{sh \times sw \times O_C \times \left\lceil \frac{F_H}{sh} \right\rceil \times \left\lceil \frac{F_W}{sw} \right\rceil \times I_C}$  having continuous memory addresses.

**Stage2** *stride-1-convolution* (Fig.6): perform stride-1 convolution on  $\nabla \mathbf{Y}$  with each  $\mathbf{C}_{y, x}$ , and finally generate  $(sh * sw)$  outputs. Each convolution is specifically with padding  $\langle \text{oph}_{y, x}, \text{opw}_{y, x} \rangle$ , and a start-position  $(ih_s, iw_s)$  corresponding to the top-left corner of an area in  $\nabla \mathbf{X}$ . Based on these start-positions,  $\nabla \mathbf{Y}$  are pruned to avoid needless calculations.

**Stage3** *gradient-composition* (Fig.7): compose all  $(sh * sw)$  outputs to get  $\nabla \mathbf{X}$ . To avoid needless calculations,  $\langle ih_s, iw_s \rangle$  is adjusted to non-negative. There is no need to check whether  $\langle ih, iw \rangle$  is in range of  $\nabla \mathbf{X}$ , when  $\langle I_H, I_W \rangle$  is integral multiple of  $\langle sh, sw \rangle$ , and the efficiency will be improved due to reduction of conditional branches.

The time-complexity of *KS-deconv* is  $\mathcal{O}(n^3)$ , and that of the naive method is  $\mathcal{O}(sh * sw * n^3)$  which is  $(sh * sw)$  times of the first. As stride increases, the gap between the two grows rapidly.

Stage2 and Stage3 are merged, so that Stage3 can directly use the outputs of Stage2 in registers. Stage1 needs  $(sh * sw * O_C * \left\lceil \frac{F_H}{sh} \right\rceil * \left\lceil \frac{F_W}{sw} \right\rceil * I_C)$  auxiliary memory to store  $\mathbf{C}$ . In most cases,  $\mathbf{C}$  takes much less memory than  $\nabla \mathbf{Y}$  and  $\nabla \mathbf{X}$ , and Stage1 has fairly smaller time-complexity than Stage2 and Stage3. So the cost of Stage1 is acceptable, and can be ignored when batchsize and feature-size are large enough. This work tried an contrast method for Stage1, where the construction of  $\mathbf{C}$  is achieved by index-conversion rather than auxiliary memory, and all 3 stages are merged to a whole; but it's slower, because of discontinuous memory-access and the overhead caused by calculating indices.

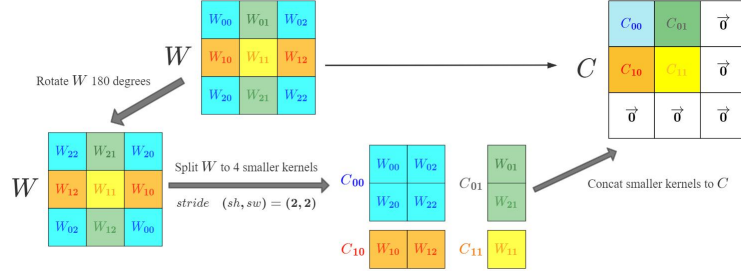


**Fig. 5.** *KS-deconv* Stage1: rotate  $W$  180 degrees. Split  $W(3 \times 3)$  to 4 smaller kernels  $C_{00}(2 \times 2)$ ,  $C_{01}(2 \times 1)$ ,  $C_{10}(2 \times 1)$  and  $C_{11}(1 \times 1)$ . Concat  $C_{00}$ ,  $C_{01}$ ,  $C_{10}$  and  $C_{11}$  to  $C(2 \times 2 \times 2 \times 2)$ , which has continuous memory addresses.

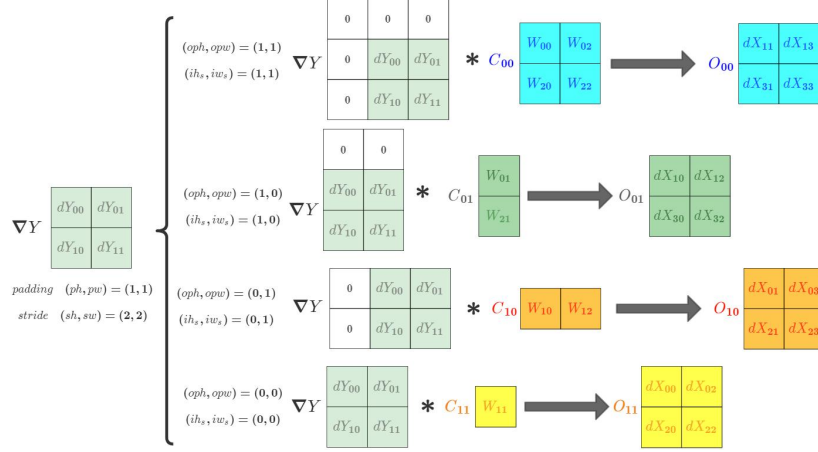


**Fig. 6.** *KS-deconv* Stage2: perform stride-1 convolution on  $\nabla Y$  with  $C_{00}$ ,  $C_{01}$ ,  $C_{10}$  and  $C_{11}$  respectively to generate 4 outputs  $O_{00}$ ,  $O_{01}$ ,  $O_{10}$  and  $O_{11}$ . The total time-complexity is 72, but only 50 calculations are necessary.

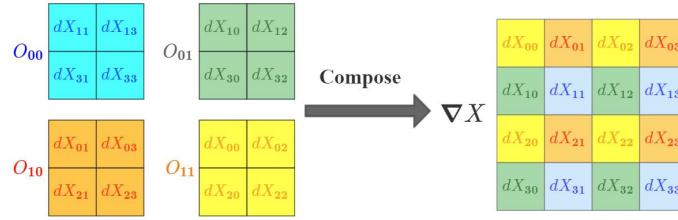


**Fig. 7.** *KS-deconv* Stage3: compose  $O_{00}$ ,  $O_{01}$ ,  $O_{10}$  and  $O_{11}$  to find  $\nabla X$ .

### C. Sk-dilated: Skip 0s in Dilated-Convolution

For deconvolution, in each patch of the sparse tensor  $\nabla Y$ , the distribution of the inserted 0s is different. But in dilated-convolution,  $\nabla Y$  performs as filters, so such 0-distribution is fixed in patches of  $X$ . Assuming  $(sh - 1)$  and  $(sw - 1)$  0s are inserted between adjacent elements of  $\nabla Y$  along the height and width axes respectively,  $(n, oh_p, ow_p, oc)$  is the index of a specific element in  $\nabla Y$ . Such element is inserted 0 if  $\langle oh_p, ow_p \rangle \% \langle sh, sw \rangle \neq \vec{0}$ , otherwise it isn't. Follow this rule, the *Sk-dilated* doesn't fill 0s to  $\nabla Y$ , but fetches element in leaping steps  $\langle sh, sw \rangle$  to generate patches, and finally reaches an equivalent result. The pseudo code of *Sk-dilated* is in Algorithm3, and a related example is in Fig.8.

The time-complexity of *Sk-dilated* is  $\Theta(n^3)$ , and that of the naive approach is  $\Theta(sh * sw * n^3)$  which is  $(sh * sw)$  times of the first. With the increase of stride, the gap between the two rapidly widens.

Through *im2col*, the *Sk-dilated-convolution* between  $X$  and  $\nabla Y$ , can be lowered to a matrix-multiply between  $A \in \mathbf{R}^{G_N \times G_K}$  and  $B \in \mathbf{R}^{G_K \times G_M}$ , where  $G_N = O_C$ ,  $G_M = F_H * F_W * I_C$  and  $G_K = N * O_H * O_W$ . But  $G_N$  and  $G_M$  don't increase with feature size, if the number of thread-blocks is determined by them alone, the GPU parallelism may be insufficient. The map-reduce model is referred to solve this problem: split  $A$  and  $B$  to  $G_Z$  segments along  $G_K$  axis, then compute these segments in parallel, finally sum up all  $G_Z$  local results to find the global result. The local computations on the  $G_Z$  segments take the most of time-complexity, so the parallelism becomes about  $G_Z$  times of the original.

The following method is used to decide  $G_Z$ . From the perspective of conv-layers, a dilated-convolution  $\gamma$  corresponds to a convolution  $\alpha$  and a deconvolution  $\beta$ . Without map-reduce, their number of thread-blocks are  $N_\alpha$ ,  $N_\beta$  and  $N_\gamma$ . Since  $N_\alpha$ ,

$N_\beta$  increase with feature size, it's feasible to let  $G_Z$  positive related to  $(N_\alpha + N_\beta)/N_\gamma$ . There also needs a lower-bound and upper-bound to limit  $G_Z$ , where the upper-bound can be determined by the number of SMs in GPU.

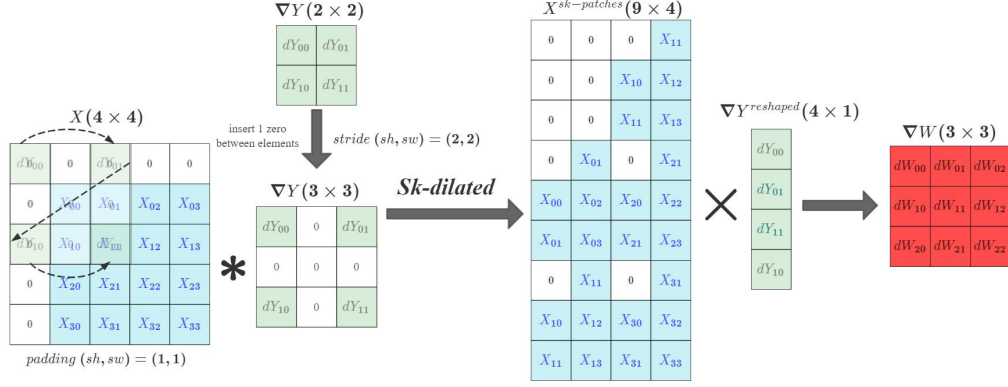


**Fig. 8.** Sk-dilated fetches elements with leaping-steps. Within the current sliding window, the elements are fetched following this sequence of indices:  $(0, 0) \rightarrow (0, 2) \rightarrow (2, 0) \rightarrow (2, 2)$ . The total time-complexity is 72, but only 50 calculations are necessary.

#### D. Combination: KS-deconv-V2 and Sk-dilated-V2

The V2 versions of KS-deconv and Sk-dilated combines the filter-trimming mechanism of ConvV2, and have better performance especially on small feature-maps, due to less time-complexity and conditional-statements. KS-deconv-V2 has 3 stages, and only the second stage is different from KS-deconv, where the stride-1 convolutions are achieved by ConvV2. The same as Sk-dilated, Sk-dilated-V2 needs ‘split- $G_K$ ’ to improve parallelism. Their pseudo code are in Algorithm 2B and Algorithm 3B. Fig.9 and Fig.10 present how they work by examples.

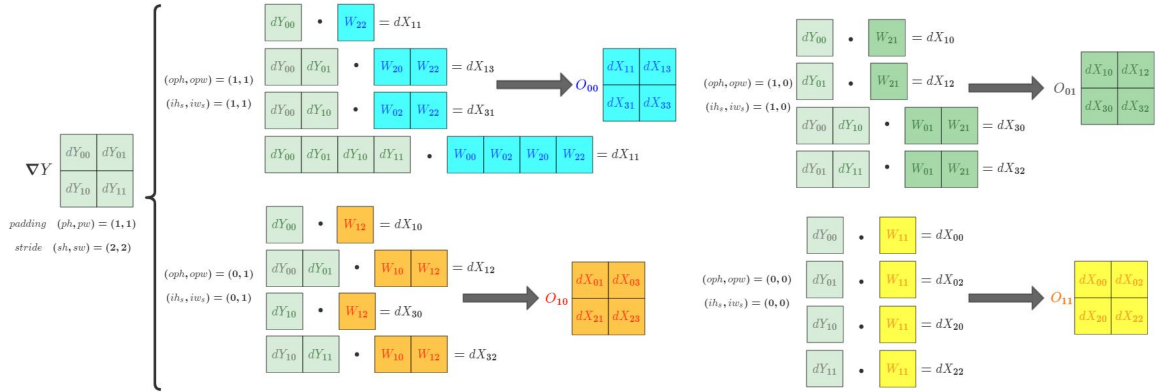


**Fig. 9.** KS-deconv-V2 Stage2 (Fig. 5 for Stage1, Fig.7 for Stage3): the stride-1 convolutions are achieved by ConvV2. The time-complexity is 50, less than 72 of KS-deconv Stage2 (Fig. 6).

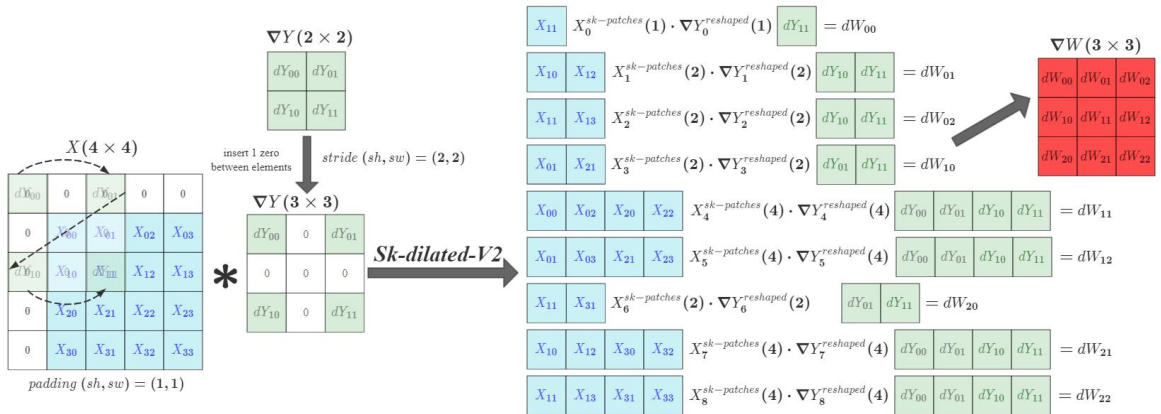


**Fig. 10.** Sk-dilated-V2: the padded 0s are excluded like ConvV2. The time-complexity is 50, less than 72 of Sk-dilated (Fig. 8).

#### E. Pseudo Code of Algorithms



Algorithm 1 <i>ConvV2</i>	Algorithm 2 <i>KS-deconv:Stage1</i>
<b>Input:</b> input-features $\mathbf{X} \in \mathbf{R}^{N \times I_H \times I_W \times I_C}$ , filters $\mathbf{W} \in \mathbf{R}^{O_C \times F_H \times F_W \times I_C}$ , stride $\langle sh \ sw \rangle$ , padding $\langle ph \ pw \rangle$ <b>Output:</b> output-features $\mathbf{Y} \in \mathbf{R}^{N \times O_H \times O_W \times O_C}$ <b>for</b> $\mathbf{Y}_{n, oh, ow, oc}$ <b>in</b> $\mathbf{Y}$ $\langle ih_s \ iw_s \rangle = \langle oh, ow \rangle \odot \langle sh \ sw \rangle - \langle ph \ pw \rangle$ $\begin{pmatrix} fh_s & fh_e \\ fw_s & fw_e \end{pmatrix} = \begin{pmatrix} \max(-ih_s, 0) & \min(I_H - ih_s, F_H) \\ \max(-iw_s, 0) & \min(I_W - iw_s, F_W) \end{pmatrix}$ $\mathbf{Y}_{n, oh, ow, oc} = \sum_{\substack{fh \in [fh_s, fh_e] \\ fw \in [fw_s, fw_e] \\ ic \in [0, I_C]}} \mathbf{X}_{n, (ih_s+fh), (iw_s+fw), ic} * \mathbf{W}_{oc, fh, fw, ic}$	<b>Input:</b> filters $\mathbf{W} \in \mathbf{R}^{O_C \times F_H \times F_W \times I_C}$ , stride $\langle sh \ sw \rangle$ <b>Output:</b> the smaller kernels $\mathbf{C} \in \mathbf{R}^{sh \times sw \times O_C \times \lceil \frac{F_H}{sh} \rceil \times \lceil \frac{F_W}{sw} \rceil \times I_C}$ <b>Initialize:</b> $\mathbf{C} = \mathbf{0}$ <b>for</b> $\mathbf{C}_{y, x}$ <b>in</b> $\mathbf{C}$ $\langle oph_{y, x} \ opw_{y, x} \rangle = \left\langle \left\lceil \frac{F_H - y}{sh} \right\rceil \quad \left\lceil \frac{F_W - x}{sw} \right\rceil \right\rangle - \vec{1}$ <b>for</b> $\mathbf{C}_{y, x, oc, ch, cw}$ <b>in</b> $\mathbf{C}_{y, x}$ $\langle fh \ fw \rangle = \langle y \ x \rangle + \langle oph_{y, x} - ch \ opw_{y, x} - cw \rangle \odot \langle sh \ sw \rangle$ $\mathbf{C}_{y, x, oc, ch, cw} = \mathbf{W}_{oc, fh, fw}$ <b>if</b> $\langle fh \ fw \rangle$ <b>in-range-of</b> $\mathbf{W}$

Algorithm 2 <i>KS-deconv:Stage2&amp;3</i>	Algorithm 2B <i>KS-deconv-V2:Stage2&amp;3</i>
<b>Input:</b> gradient of output-features $\nabla \mathbf{Y} \in \mathbf{R}^{N \times O_H \times O_W \times O_C}$ , the smaller kernels $\mathbf{C} = \mathbf{0} \in \mathbf{R}^{sh \times sw \times O_C \times \lceil \frac{F_H}{sh} \rceil \times \lceil \frac{F_W}{sw} \rceil \times I_C}$ stride $\langle sh \ sw \rangle$ , padding $\langle ph \ pw \rangle$ <b>Output:</b> gradient of input-features $\nabla \mathbf{X} \in \mathbf{R}^{N \times I_H \times I_W \times I_C}$ <b>for</b> $\mathbf{C}_{y, x}$ <b>in</b> $\mathbf{C}$ $\langle ih_s \ iw_s \rangle = \langle y \ x \rangle - \langle ph \ pw \rangle$ $\langle ih_s \ iw_s \rangle += (1_{ih_s < 0} \ 1_{iw_s < 0}) \odot \left\langle \left\lceil \frac{-ih_s}{sh} \right\rceil \quad \left\lceil \frac{-iw_s}{sw} \right\rceil \right\rangle \odot \langle sh \ sw \rangle$ <b>for</b> $\langle n \ u \ v \ ic \rangle = \vec{0}$ <b>to</b> $\langle N \ \lceil \frac{I_H}{sh} \rceil \ \lceil \frac{I_W}{sw} \rceil \ I_C \rangle - \vec{1}$ $\langle ih \ iw \rangle = \langle u \ v \rangle \odot \langle sh \ sw \rangle + \langle ih_s \ iw_s \rangle$ $\langle oh_s \ ow_s \rangle = \left\langle \left\lceil \frac{ih+ph-y}{sh} \right\rceil \quad \left\lceil \frac{iw+pw-x}{sw} \right\rceil \right\rangle - \langle oph_{y, x} \ opw_{y, x} \rangle$ <b>continue if</b> $\langle ih \ iw \rangle$ <b>not in-range-of</b> $\nabla \mathbf{X}$ $\nabla \mathbf{X}_{n, ih, iw, ic} = \mathbf{0}$ <b>for</b> $\mathbf{C}_{y, x, oc, ch, cw, ic}$ <b>in</b> $\mathbf{C}_{y, x}$ : $\langle oh \ ow \rangle = \langle oh_s \ ow_s \rangle + \langle ch \ cw \rangle$ <b>continue if</b> $\langle oh \ ow \rangle$ <b>not in-range-of</b> $\nabla \mathbf{Y}$ $\nabla \mathbf{X}_{n, ih, iw, ic} += \nabla \mathbf{Y}_{n, oh, ow, oc} * \mathbf{C}_{y, x, oc, ch, cw, ic}$	<b>Input:</b> gradient of output-features $\nabla \mathbf{Y} \in \mathbf{R}^{N \times O_H \times O_W \times O_C}$ , the smaller kernels $\mathbf{C} = \mathbf{0} \in \mathbf{R}^{sh \times sw \times O_C \times \lceil \frac{F_H}{sh} \rceil \times \lceil \frac{F_W}{sw} \rceil \times I_C}$ stride $\langle sh \ sw \rangle$ , padding $\langle ph \ pw \rangle$ <b>Output:</b> gradient of input-features $\nabla \mathbf{X} \in \mathbf{R}^{N \times I_H \times I_W \times I_C}$ <b>for</b> $\mathbf{C}_{y, x}$ <b>in</b> $\mathbf{C}$ $\langle C_H^{y, x} \ C_W^{y, x} \rangle = \left\langle \left\lceil \frac{F_H - y}{sh} \right\rceil \quad \left\lceil \frac{F_W - x}{sw} \right\rceil \right\rangle$ $\langle ih_s \ iw_s \rangle = \langle y \ x \rangle - \langle ph \ pw \rangle$ $\langle ih_s \ iw_s \rangle += (1_{ih_s < 0} \ 1_{iw_s < 0}) \odot \left\langle \left\lceil \frac{-ih_s}{sh} \right\rceil \quad \left\lceil \frac{-iw_s}{sw} \right\rceil \right\rangle \odot \langle sh \ sw \rangle$ <b>for</b> $\langle n \ u \ v \ ic \rangle = \vec{0}$ <b>to</b> $\langle N \ \lceil \frac{I_H}{sh} \rceil \ \lceil \frac{I_W}{sw} \rceil \ I_C \rangle - \vec{1}$ $\langle ih \ iw \rangle = \langle u \ v \rangle \odot \langle sh \ sw \rangle + \langle ih_s \ iw_s \rangle$ $\langle oh_s \ ow_s \rangle = \left\langle \left\lceil \frac{ih+ph-y}{sh} \right\rceil \quad \left\lceil \frac{iw+pw-x}{sw} \right\rceil \right\rangle - \langle oph_{y, x} \ opw_{y, x} \rangle$ $\begin{pmatrix} ch_s & ch_e \\ cw_s & cw_e \end{pmatrix} = \begin{pmatrix} \max(-oh_s, 0) & \min(O_H - oh_s, oph_{y, x}) \\ \max(-ow_s, 0) & \min(O_W - ow_s, opw_{y, x}) \end{pmatrix}$ <b>continue if</b> $\langle ih \ iw \rangle$ <b>not in-range-of</b> $\nabla \mathbf{X}$ $\nabla \mathbf{X}_{n, ih, iw, ic} = \sum_{\substack{ch \in [ch_s, ch_e] \\ cw \in [cw_s, cw_e] \\ ic \in [0, I_C]}} \nabla \mathbf{Y}_{n, (oh_s+ch), (ow_s+cw), oc} * \mathbf{C}_{y, x, oc, ch, cw, ic}$

Algorithm 3 <i>Sk-dilated</i>	Algorithm 3B <i>Sk-dilated-V2</i>
<b>Input:</b> gradient of output-features $\nabla \mathbf{Y} \in \mathbf{R}^{N \times OH \times OW \times OC}$ , input-features $\mathbf{X} \in \mathbf{R}^{N \times IH \times IW \times IC}$ , stride $\langle sh \ sw \rangle$ , padding $\langle ph \ pw \rangle$ <b>Output:</b> gradient of filters $\nabla \mathbf{W} \in \mathbf{R}^{OC \times FH \times FW \times IC}$ <b>for</b> $\nabla \mathbf{W}_{oc, fh, fw, ic}$ <b>in</b> $\nabla \mathbf{W}$ $\langle ih_s \ iw_s \ \nabla \mathbf{W}_{oc, fh, fw, ic} \rangle = \langle fh - ph \ fw - pw \ 0 \rangle$ <b>for</b> $\nabla \mathbf{Y}_{n, oh, ow, oc}$ <b>in</b> $\nabla \mathbf{Y}$ $\langle ih \ iw \rangle = \langle oh, ow \rangle \odot \langle sh \ sw \rangle + \langle ih_s \ iw_s \rangle$ <b>continue if</b> $\langle ih \ iw \rangle$ <b>not in-range-of</b> $\mathbf{X}$ $\nabla \mathbf{W}_{oc, fh, fw, ic} += \mathbf{X}_{n, ih, iw, ic} * \nabla \mathbf{Y}_{n, oh, ow, oc}$	<b>Input:</b> gradient of output-features $\nabla \mathbf{Y} \in \mathbf{R}^{N \times OH \times OW \times OC}$ , input-features $\mathbf{X} \in \mathbf{R}^{N \times IH \times IW \times IC}$ , stride $\langle sh \ sw \rangle$ , padding $\langle ph \ pw \rangle$ <b>Output:</b> gradient of filters $\nabla \mathbf{W} \in \mathbf{R}^{OC \times FH \times FW \times IC}$ <b>for</b> $\nabla \mathbf{W}_{oc, fh, fw, ic}$ <b>in</b> $\nabla \mathbf{W}$ $\langle ih_s \ iw_s \rangle = \langle fh - ph \ fw - pw \rangle$ $\begin{pmatrix} oh_s & oh_e \\ ow_s & ow_e \end{pmatrix} = \begin{pmatrix} \max(\left\lceil \frac{-ih_s}{sh} \right\rceil, 0) & \min(O_H, \left\lceil \frac{I_H - ih_s}{sh} \right\rceil) \\ \max(\left\lceil \frac{-iw_s}{sw} \right\rceil, 0) & \min(O_W, \left\lceil \frac{I_W - iw_s}{sw} \right\rceil) \end{pmatrix}$ $\nabla \mathbf{W}_{oc, fh, fw, ic} = \sum_{\substack{oh \in [oh_s, oh_e] \\ ow \in [ow_s, ow_e] \\ n \in [0, N]}} \mathbf{X}_{n, (ih_s+oh*sh), (iw_s+ow*sw), ic} * \nabla \mathbf{Y}_{n, oh, ow, oc}$

## F. GPU Optimizations

Over 100 kernel functions have been designed for *C-K-S*. Some are general solutions to assure performance, while some are specialized to achieve higher performance in specific situations. For convenience, they are classified and integrated, to make a higher-level encapsulation [10].

The integral divide and remainder operations perform much slower than the floating-operations on GPUs, so their usage should be minimized. The bit-wise operators are used to replace them. Some results are pre-calculated, stored in constant memory to maximize the broadcast, and retrieved during calculation.

GPUs are not good at executing conditional structures, because of their single-instruction-multiple-data (SIMD) nature. Therefore, some conditional-statements are replaced with equivalent tables and expressions, and some fixed-loop are unrolled to minimize judgement-statements.

The last dimension of tensors are padded to 4x implicitly, and some memory operation are merged through vector-types, in order to improve the bandwidth by using 128bit as the minimum unit for memory access.

For dense kernels, *im2col*, *reshape*, *transpose*, *padding*, *etc* operators are integrated to them, and achieved through index-conversion without auxiliary memory. Double-buffer shared-memory is used to hasten data loading. Each thread executes a big batch of instructions per round to hide memory access. Some statements are reordered to reduce the consumption of registers.

#### IV. EXPERIMENTS

In this work, the GPU implementations of *C-K-S-V2* (*ConvV2*, *SK-deconv-V2*, *Sk-dilated-V2*) are improved from cu32 of Dragon-Alpha [10] [23]. This section discusses their performance and variation tendencies. PyTorch (1.12.1) [11] is used as a baseline for comparison, as its underlying GPU library cuDNN [7] has been extremely optimized. *ConvV2* is evaluated from the perspective of forward propagation, while *KS-deconv-V2* and *Sk-dilated-V2* are in a view of backward propagation. To understand the overall performance of *C-K-S*, please refer the experimental datas of Dragon-Alpha [10].

##### A. Methods

For each member of *C-K-S-V2*, 2 test-sets with different filter-size are provided, and each test-set contains 8 test-cases. From the 1<sup>st</sup> to the 8<sup>th</sup> test-case, the feature-size goes smaller, but channels and batchsize become bigger. The stride or dilation is 2 to introduce sparse tensor.

The operators were tested on RTX 3060ti GPU with CUDA 11.5 in *float32* data-type. All calculations were performed on GPU, and there was no data transmission between GPU and CPU. At the same time, only 1 operator was executed to grasp all GPU resource, while the interference from other programs was minimized, and the size of input data is large enough to ensure parallelism. To maximize PyTorch's speed, it pre-allocated enough memory space before loops of executing a specific convolutional operator; it didn't do any rotate or transpose operations to change the arrangement of tensors, but just executed convolutional operators.

Each operator was executed 1000 times in succession for each of their test-cases, and the *cudaDeviceSynchronize()* was called to ensure the completion of each execution. The total execution time was averaged to find the speed of floating-point-operation, and the unit is GFlop/s ( $10^9$  *float32* operations per second). The formulas for time-complexity of convolutional operators are listed in TABLE II.

TABLE II  
FORMULAS FOR TIME-COMPLEXITY

Formula	Explanation
$T_{Conv} = 2 * (O_C * N * O_H * O_W * F_H * F_W * I_C)$	Time-complexity of 2D-Convolution.
$T_{Deconv} = 2 * (I_C * N * I_H * I_W * F_H * F_W * O_C)$	Time-complexity of 2D-Deconvolution.
$T_{Dilated} = 2 * (O_C * F_H * F_W * I_C * O_H^p * O_W^p)$	Time-complexity of 2D-Dilated-Convolution.
$O_H^p = O_H + (O_H - 1) * (sh - 1)$	The height of $\nabla Y$ with inserted $(sh - 1)$ 0s.
$O_W^p = O_W + (O_W - 1) * (sw - 1)$	The width of $\nabla Y$ with inserted $(sw - 1)$ 0s.



## B. Results

The line-charts are used to demonstrate the variation of speed under different tensor shapes. The results of convolution are shown in Fig. 11-12, where the ‘\*’ means excluding the time of changing the dimension order of  $W$  to  $F_H \times F_W \times I_C \times O_C$ . Fig.13-14 present the results of deconvolution, and Fig.15-16 list the results of dilated-convolution.

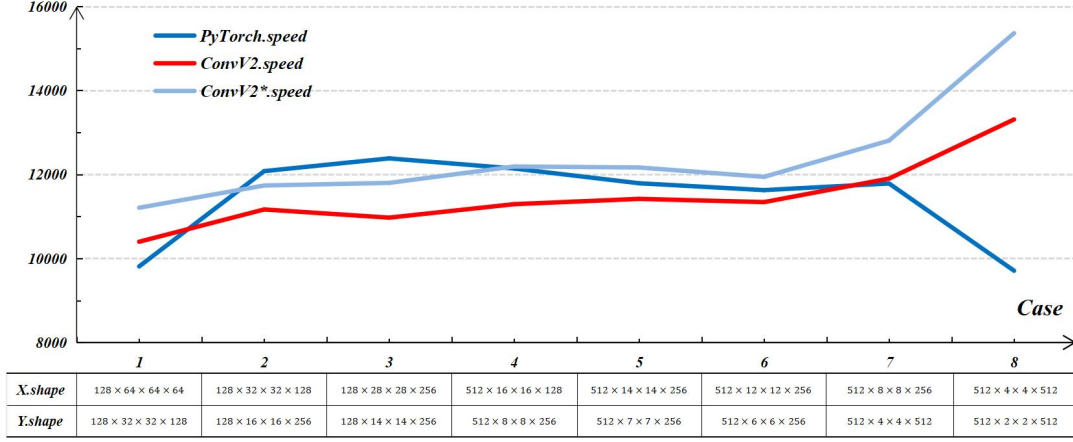


Fig. 11. Convolution with  $\langle F_H F_W \rangle = \vec{3}$ , stride = 2, padding = 1.

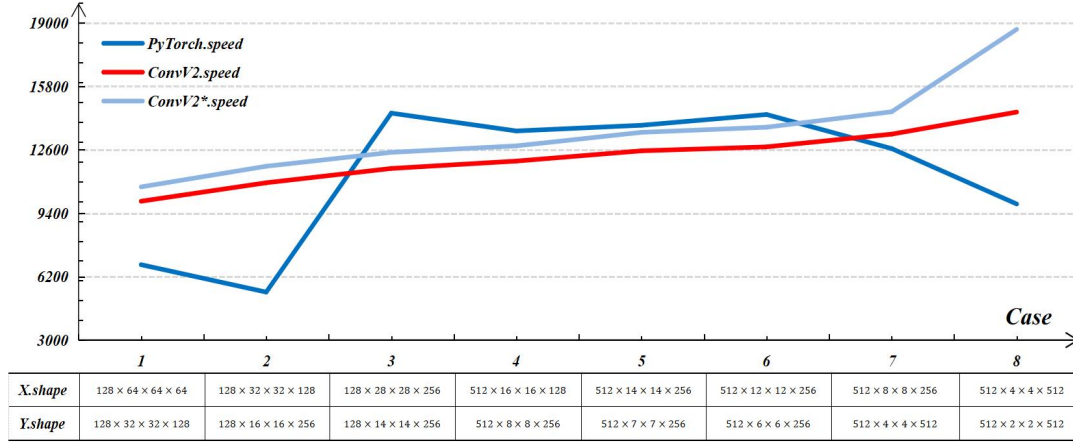


Fig. 12. Convolution with  $\langle F_H F_W \rangle = \vec{5}$ , stride = 2, padding = 2.

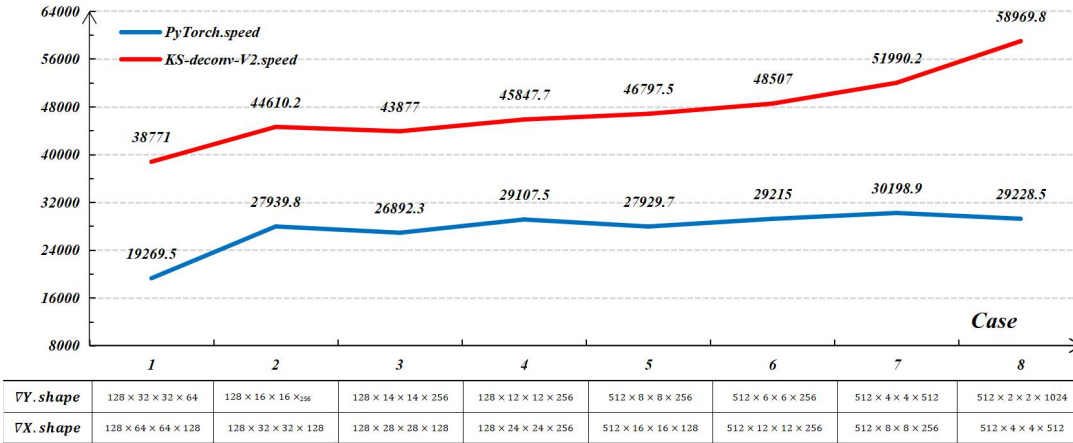


Fig. 13. Deconvolution with  $\langle F_H F_W \rangle = \vec{3}$ , stride = 2, padding = 1.

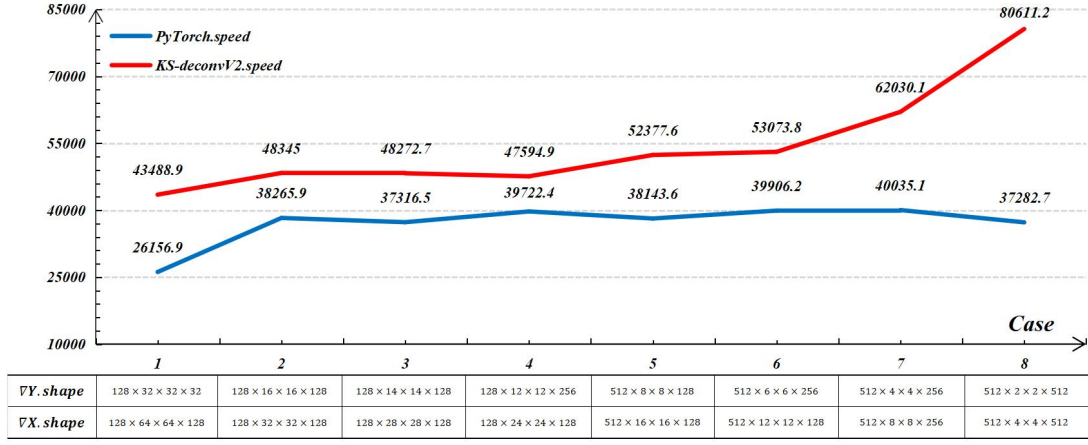


Fig. 14. Deconvolution with  $\langle F_H F_W \rangle = \vec{5}$ ,  $stride = 2$ ,  $padding = 2$ .

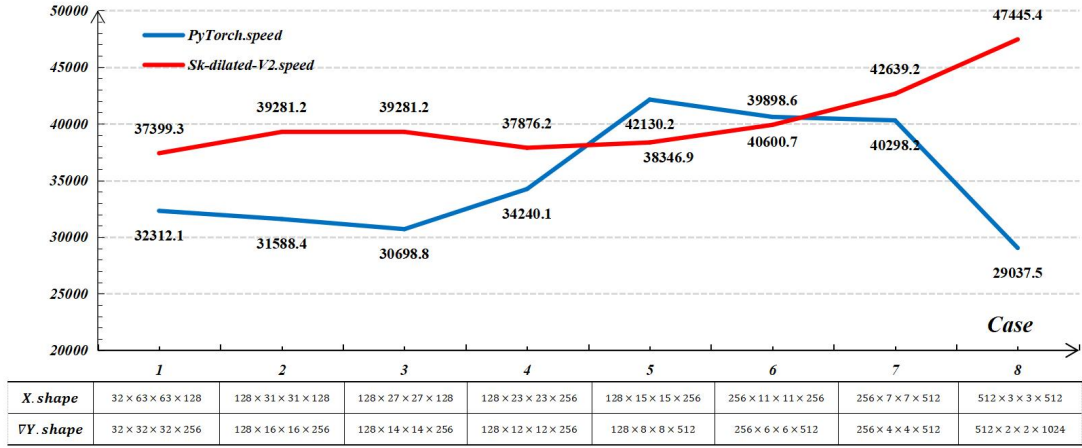


Fig. 15. Dilated-Convolution with  $\langle F_H F_W \rangle = \vec{3}$ ,  $dilated = 2$ ,  $padding = 1$ .

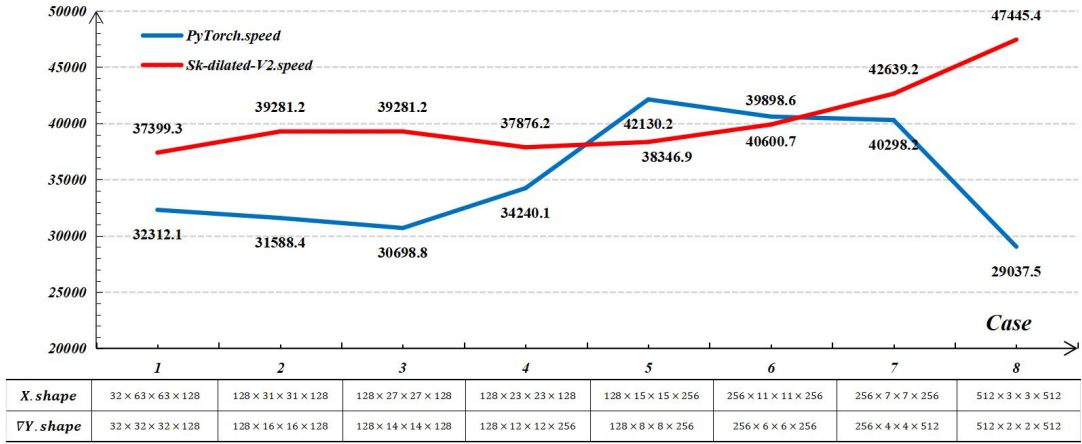


Fig. 16. Dilated-Convolution with  $\langle F_H F_W \rangle = \vec{5}$ ,  $dilated = 2$ ,  $padding = 2$ .

### C. Discussions

In deconvolution, *KS-deconv* has better performance in all 16 cases than PyTorch. In convolution and dilated-convolution, PyTorch is faster in the middle cases, while the other situations are opposite. In most DNNs for image-processing, the deeper layers with big channels and smaller feature-size, usually causes the majority of time-complexity. Therefore, cuDNN made full optimizations for them, to be more efficient than this work's implementations. But due to filter-trimming, the speed of *ConvV2* and *Sk-dilated-V2* finally exceeds that of PyTorch. Conclusively, these comparisons prove the effectiveness of this work's GPU implementations of *C-K-S-V2*.

Benefiting from filter-trimming, *C-K-S-V2* has faster speed with smaller feature-size in general, since more padded 0s are excluded. Due to downsampling, in all test-cases, the size of output-feature-map is smaller than that of input-feature-map, so the filter-trimming mechanism plays a more significant role in deconvolution, that leads a higher speed.

In deconvolution and dilated-convolution,  $\nabla Y$  expands nearly 4 times because of the inserted 0s. But these 0s are skipped through *KS-deconv* and *Sk-dilated*, resulting in the following two gains: first, the actual time-complexity is only about 25% of that in theory; second, there is no sparse tensor involved in calculation, therefore, the design pattern of *ConvV2*'s kernel functions for dense computing, can be naturally migrated to those of *KS-deconv* and *Sk-dilated*, so that they can efficiently utilize the GPU to a similar extent. That's why the speed of *KS-deconv* and *Sk-dilated* is close to 4 times of *ConvV2*'s.

But it's difficult to exceed such '4 times', owing to their complicity compared to *ConvV2*. *KS-deconv* needs additional resources to reconstruct the filters, and more registers for intermediate variables, which lowers the parallelism of dense kernels due to less active threads. The *Sk-dilated* relies on 'split- $G_K$ ' to obtain sufficient parallelism, that inevitably causes certain expenses; in addition, its memory access is less continuous with larger spans, that hurts the hit-radio of L2-cache.

The heaviest kernel functions of *C-K-S-V2* refers the *implicit-GEMM* approach, and are selected to handle large-scale data, so their performance remains stable in all test cases. When handling large-scale data, the speed of *ConvV2* can improve by 5% to 10%, without the time of dimension reordering of  $W$ , and such reordering can be avoided with better tensor arrangement, or be hidden in the parallel execution of multi operators. When using *ConvV2* or *KS-deconv* to perform one-way propagation, it's able to reconstruct the filters before loops of convolutional operators, as it can further reduce the computational time.

## V. CONCLUSION

This paper discusses the motivation, 2D-algorithms and implementations of *C-K-S*, and verifies its effectiveness through experiments with comparison to PyTorch. The *C-K-S* skips 0-calculations in two ways: avoid the inserted 0s in  $\nabla Y$  to convert it back to dense tensor, and exclude the padded 0s by filter-trimming. *C-K-S* lowers the time-complexity in theory, and has adaptability to GPU to achieve high-performance, so that it has the potential to break the upper-limit of devices' compute capability.

Certain optimizations for GPUs were done in this work, but not full optimization oriented at the Ampere architecture [23] to extremely utilize the hardware. The bank-conflict on shared-memory hasn't been thoroughly solved, that lowers the performance of dense kernels. All GPU programming is by C++ without integrated ptx-codes, and the executable files are directly generated by the compiler with no fine-tuning on sass-codes. For elements fetching of convolutional operators, the memory bandwidth was improved, but the overlaps between patches haven't been fully used. Further enhancements can be made according to the aforementioned defects.

## REFERENCES

- [1] I. Goodfellow, T. Bengio, and A. Courville, "Deep Learning," [Online]. Available: <https://www.deeplearningbook.org>.
- [2] A. Krizhevsky, I. Sutskever and G. E. Hinton, "Imagenet classification with deep convolutional neural networks," in *Proc. NIPS*, 2012, pp. 1097-1105.
- [3] K. Simonyan and A. Zisserman, "Very Deep Convolutional Networks for Large-Scale Image Recognition," [Online]. Available: <https://arxiv.org/abs/1409.1556>.
- [4] C. Szegedy, W. Liu, Y. Jia, *et al.*, "Going deeper with convolutions," [Online]. Available: <https://arxiv.org/abs/1409.4842v1>
- [5] K. He, X. Zhang, S. Ren, and J. Sun, "Deep residual learning for image recognition". in *Proc. CVPR*, Jun. 2016, pp. 770-778.
- [6] Z. Liu, H. Mao, C. Feichtenhofer, *et al.*, "ConvNext: A ConvNet for 2020s," [Online]. Available: <https://arxiv.org/abs/2201.03545>.
- [7] Travis Oliphant. "NumPy: A guide to NumPy". [Online] Available: <https://numpy.org>.
- [8] S. Chetlur, C. Woolley, P. Vandermersc, J. Cohen and E. Shelhamer, "cuDNN Efficient Primitives for Deep Learning", [Online]. Available: <https://arxiv.org/abs/1410.0759v3>.
- [9] Tencent. "NCNN," [Online]. Available: <https://github.com/Tencent/ncnn>.
- [10] Z. Zhang, Q. Wang and P. Zhang. "Dragon-Alpha&cu32: A Java-based Tensor Computing Framework with its High-Performance CUDA Library". [Online]. Available: <https://arxiv.org/abs/2305.08819>.
- [11] A. Paszke, S. Gross, F. Massa, *et al.*, "PyTorch: An Imperative Style, High-Performance Deep Learning Library," [Online]. Available: <https://arxiv.org/abs/1912.01703v1>.
- [12] NVIDIA, "CUDA C Programming Guide," [Online]. Available: <https://docs.nvidia.com/cuda/cuda-c-programming-guide>.

- [13] NVIDIA, “CUDA C Best Practices Guide,” [Online]. Available: <https://docs.nvidia.com/cuda/cuda-c-best-practices-guide>.
- [14] D. E. Rumelhart, G. E. Hinton, *et al.*, “Learning Representations by Back-Propagating errors,” *Nature*, vol. 323, no. 6088, pp. 533–536, Oct. 1986, doi: 10.1038/323533a0.
- [15] J. Chang, K. Kang and S. Kang, “An Energy-Efficient FPGA-Based Deconvolutional Neural Networks Accelerator for Single Image Super-Resolution,” in *IEEE Transactions on Circuits and Systems for Video Technology*, vol. 30, no. 1, pp. 281-295, Jan. 2020, doi: 10.1109/TCSVT.2018.2888898.
- [16] K. Chang and T. Chang, “Efficient Accelerator for Dilated and Transposed Convolution with Decomposition,” 2020 *IEEE ISCAS*, Seville, Spain, 2020, pp. 1-5, doi: 10.1109/ISCAS45731.2020.9180402.
- [17] A. M. Vadakkevedu, D. Mandal, P. Ramachandran and N. Chandrachoodan, “Split-Knit Convolution: Enabling Dense Evaluation of Transpose and Dilated Convolutions on GPUs,” 2022 *IEEE 29th HiPC*, Bengaluru, India, 2022, pp. 1-10, doi: 10.1109/HiPC56025.2022.00014.
- [18] L. Orosa, S. Koppula, Y. Umuroglu, *et. al.*, “EcoFlow: Efficient Convolutional Dataflows for Low-Power Neural Network Accelerators,” arXiv e-prints, Feb. 2022.
- [19] A. Kerr, H. Wu, M. Gupta, D. Blasig, *et. al.*, “CUTLASS,” 2022. [Online]. Available: <https://github.com/NVIDIA/cutlass>
- [20] Y. Jia, E. Shelhamer, J. Donahue, *et al.*, “caffe: Convolutional architecture for fast feature embedding,” [Online]. Available: <https://arxiv.org/abs/1408.509>.
- [21] A. Krizhevsky. “cuda-convnet2,” [Online]. Available: <https://code.google.com/p/cuda-convnet2/>.
- [22] Zhiyi Zhang, “Dragon-Alpha”. [Online]. Available: <https://github.com/GilgameshXYZ123/Dragon-Alpha>.
- [23] NVIDIA, “NVIDIA Turing GPU Architecture”. [Online]. Available: <https://images.nvidia.com/aem-dam/en-zz/Solutions/design-visualization/technologies/turing-architecture/NVIDIA-Turing-Architecture-Whitepaper.pdf>